Journal Pre-proof

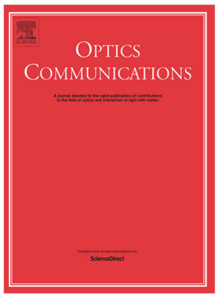

Liquid-crystal q-plates with a phase core to generation vortex beams with controllable number of singularities

E. Melnikova, D. Gorbach, S. Slussarenko Sr., A. Muravsky,
A. Tolstik, S. Slussarenko Jr.

PII: S0030-4018(22)00435-7
DOI: https://doi.org/10.1016/j.optcom.2022.128661
Reference: OPTICS 128661

To appear in: *Optics Communications*

Received date : 27 February 2022
Revised date : 15 June 2022
Accepted date : 16 June 2022

Liquid-crystal q-plates with a phase core to generation vortex beams with controllable number of singularities

E. Melnikova[1], D. Gorbach[1], S. Slussarenko Sr.[1], A. Muravsky[1], A. Tolstik[1], S. Slussarenko Jr.[2]

[1]Physics Department, Belarusian State University, Nezavisimosti Avenue 4, 220030 Minsk, Belarus
[2]Centre for Quantum Dynamics and Centre for Quantum Computation and Communication Technology, Griffith University, Brisbane, Queensland 4111, Australia
*Corresponding author: Slussarenko@yahoo.com

Abstract: Based on the method of azo dye photoalignment, electrically controlled liquid crystal (LC) q-plates for the generation of a given number of polarization and phase optical singularities have been designed. The results of experimental studies of polarization and phase characteristics of the generated singular beams are in good agreement with the proposed theoretical model. The proposed devices can be adapted for a variety of problems of modern photonics, including implementation of structured illumination microscopy, information coding, optical security technology, microrheology etc.

Introduction

Light beams with complex amplitude, phase, and polarization topologies are of great interest nowadays. They have found wide application in optical communication systems [1], optical capture and manipulation of microobjects [2], recording of singular holograms [3], for efficient material processing [4], in atmospheric research [5], etc.

Among such beams, optical and vector vortices are distinguished. Optical vortices are characterized by helicoidal twisting of the wave phase around the propagation axis [6–8]. The 2π azimuthal phase winding per oscillation period is defined as the topological charge l of the beam [7]. In the area of phase uncertainty, the field amplitude becomes equal to zero. Vector vortices, in turn, characterized by an uncertain polarization state and are beams with isolated intensity dips in the profile, around which radial, azimuthal or radial-azimuthal polarization is established [7–13]. The topological charge l_p of such beams is defined as the number of turns of the polarization azimuth per oscillation period [11].

To obtain singular light beams various technologies are used: optical plates with smoothly varying thickness, spatial LC light modulators, diffraction elements, etc. [6, 12–15]. Q-plates as optical elements with spatially structured anisotropy are a sphere of a great interest [16].

The significant value of optical anisotropy and the ability to control it under low operating voltages ensured the effective use of LC in systems for information display, light beam control, integral optics and nanophotonics [17–23], as well as a promising material for fabricating q-plates [24–26].

These q-plates are a LC cell: a layer of LC is placed between two transparent electrode plates which define structured azimuthal distribution of the local optical axis in the cell plane. The q-plate characterized by the topological charge q, which determines the rate of change in the orientation of the optical axis with respect to the azimuth angle. At that local director distribution in the cell plane is given as:

$$\alpha(\rho, \varphi) = q\varphi + \alpha_0, \tag{1}$$

where φ, ρ – polar coordinates, α_0 – initial angle of the director orientation.

Azimuthally anisotropic LC elements, with phase retardation between ordinary and extraordinary beams are equal to $\Delta\Phi = \pi(2m + 1)$, are functioning as a half-wave plate. On passage of Gaussian circularly polarized light with the spin angular momentum $\sigma = \pm 1$, the formed optical vortices have the topological charge $l = \sigma 2q$ and the inverted sign of the spin angular momentum [24]. On linear polarization of the input optical beam, q-plates form a beam with structured orientation of linear polarization in its cross section, defined as $\theta = 2\ (\alpha - \beta)$, where α – LC director orientation angle (1) and β – orientation angle of the input linear polarization [25, 26]. The optical fields formed in this way contain a region with an undefined polarization state, known as a V- point [27]. For a q-plate with a topological charge $q = 0{,}5$ light beams with azimuthal or radial polarization are realized; for $q \geq 1$ more complex polarization singularities characterized by a topological charge $l_p = 2q$ are observed. The possibility of creating light beams with a complex spatial structure, including beams containing a given number of singularities, has also attracted the attention of researchers [28–30]. The possibility of realizing the optical capture of several particles using such fields can be used, for example, in microreology [7, 30].

There are various ways to set the alignment of the director in LC elements: mechanical rubbing and photoalignment. The method of mechanical rubbing is limited by the topological charge of the q-plate ($q = 1$) [14]. The sector photoalignment technique [31–33] allows one to create elements with any value of charge q, including fractional, however it limited by the azimuthal topology of the local optical axis orientation. It is possible to use the method of dynamic microlithography to create more complex local optical axis distribution structure. These elements allow forming the beams with a complex distribution of amplitude, phase, and polarization characteristics, thereby broadening the possibilities of their application. However, this method is technically complicated due to using a multi-stage exposure [34–36].

We propose a method combining the simplicity of sectoral photoalignment and the possibility of forming a complex distribution of light field characteristics with a controlled number of singularities. An additional advantage is a significant reduction in the radiation power and the time of creating an optical element in comparison with, for example. [31].

Scheme for recording q-plates with a central phase core

Fabrication of typical q-plates by the traditional photoalignment technique [31] requires ideal centering of the optical scheme so that the LC orientation singularity zone converges to a point on the orientant surface and translates in the LC layer volume strictly along the optical axis of the exposure system (ω=0 in Fig. 1). In this case a q-plate forms optical vortices with topological charge l, definitely determined by the plate charge value $l = \pm 2q$, with a single intensity dip.

Displacement of the Wedge-Shaped Diaphragm by a certain distance from the rotation axis (ω>0 in Fig. 1), lead to formation in the center of the LC based q-plate a zone where the orientation of the LC director is determined by homogeneous boundary conditions on the substrates – the phase core. Such q-plates will form as $N = 2q$ optical singularities with a topological charge $l = 1$.

To create q-plates with a phase core we used a setup schematically shown in Figure 1. Collimated radiation of a light-emitting diode (LED), with the wavelength 440-460 nm, transmitted through a linear polarizer illuminated the wedge-shaped diaphragm. Its image is projected into the LC cell plane with the help of a system of two lenses. Thin film (20-30 nm thick) of the AtA-2 azo dye [37–39] formed the initial distribution of the director of a nematic LC in the element. Owing to the use of this azo dye, a new mechanism of LC photoinduced orientation was proposed on the basis of photoinduced hole dipoles [40], offering a high level of photosensitivity and a high energy of cohesion with LC molecules [41, 42], high thermo- and photostability [37]. The power density of exposing polarized radiation was 15 mW/cm^2. The formation of a phase core in the central part of the LC element was attained by shift of the central part of the wedge-shaped diaphragm to the distance ω from the rotation axis. At that, in the centre of an element the boundary conditions at the photoorientant surface form the phase core with the diameter 2ω.

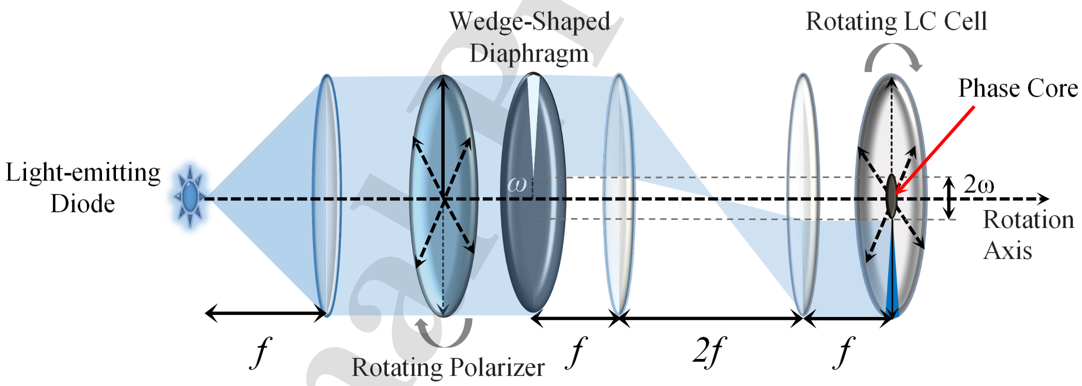

Figure 1– Schematic of an experimental setup for recording of q-plates with a central phase core.

Computer control of the LED on/off switching mode, the rotation angle for a polarizer and an LC cell allowed making q-plates with different topological charges. Owing to the angular diaphragm size in 2°, there was a possibility to form an LC element with 180 sectors providing the orientation of the LC director in line with formula (1). Exposure time for one sector was 20 seconds. Total exposure time for the LC cell was 1 hour. The cell was filled with NLC 1289 (prototype E7), Δn = 0.18, with the LC cell film thickness d =7 μm.

Usage of the AtA-2 azo dye made it possible to reduce the required absorbed dose value by more than an order of magnitude (for the method given in [31], the power density of exposing radiation was 180 mW/cm^2, and the recording time – 2 hours).

***Q*-Plates with phase core**

Experimental studies have been performed using the fabricated *q*-plates with the topological charges q = 0.5, q = 1, and q =1.5 and with a phase core in the central part of the element. Figure 2 shows the director distribution topology in the plane of LC elements (*a*) as well as the photographs for *q*-plates at crossed polarizers (*b*), CCD images for the intensity profiles of the formed phase vortices (*c*), and the corresponding interference patterns of phase vortices with a plane coherent wave (*d*). Singular beams were formed with the use of a helium-neon laser (λ = 0,633 μm).

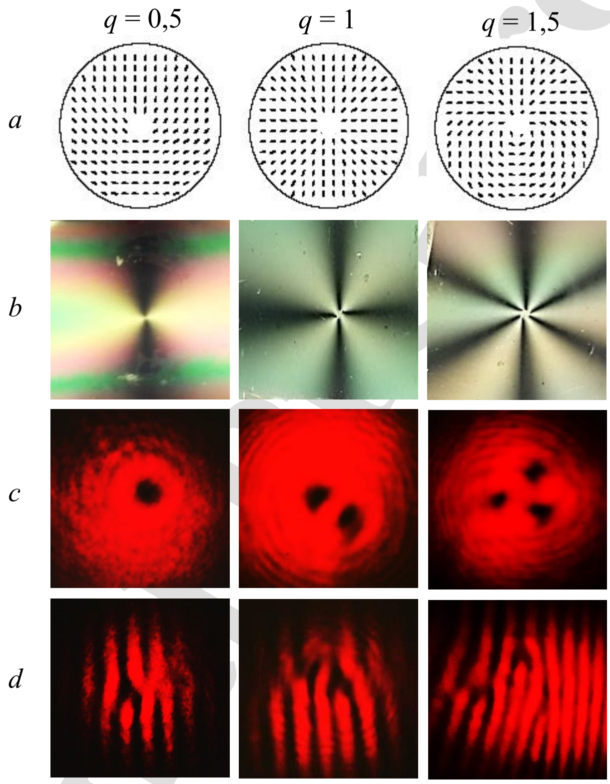

Figure 2 – *q*-plates with a phase core and with different topological charges.
(*a*) – LC-director orientation topology; (*b*) – polarization images (in white light);
(*c*) – photographs of the intensity profiles for a phase vortex;
(*d*) –interference patterns with a plane wave.

As seen from experimental data (Fig.2 *a, b*), the orientation of the LC director differs from the condition (1) in the region of the phase core. This part of a LC element leads to the transformation of laser radiation into an optical vortex by the way different from the typical one for *q*-plates [31]. In this case, instead of a doughnut beam, one can observe several singularities in intensity profile. At this observed number of phase singularities with the topological charge $|l| = 1$ is definitively given by the expression $N = 2q$. To illustrate, a plate with the charge q=0.5 forms a single optical vortex with the charge $|l| = 1$, a plate with q=1 forms two vortices, whereas a plate with q = 1.5 – three one. To control the charge of the formed vortexes, we use a Mach-Zender interferometer (Fig.2 *c*, *d*).

Theoretical model

Let us interpret the experimental results obtained for the transformation of a Gaussian beam passing through the designed q-plates, in terms of the effect exerted by a nonsingular component (Gaussian beam transmitted through the phase core region of a q-plate) or by noise in a field of optical singularities. It is known that the presence of noise in a singular light field results in breaking of high-order optical vortices into several vortices with the charge $|l| = 1$ [43–45].

Spatial distribution of an electromagnetic field of singular optical beams is well described by the so-called hypergeometric Gaussian beams [46, 47]. For simplicity, we limit to the Laguerre-Gauss mode approximation [44]. In this case complex amplitude LG_l of a beam in the polar coordinates is as follows:

$$LG_l = C_l \vec{e_j} \rho^{|l|} e^{il\varphi - \rho^2}, \tag{2}$$

where ρ – polar radius, φ – angle (in Cartesian coordinates: $\rho = \sqrt{x^2 + y^2}$, $\varphi = \mathrm{ArcTan}[x, y]$), l – vortex topological charge, C_l – normalized amplitude of the LG beam, $\vec{e_j}$ – base polarization vector (the indices R, L are associated with right- and left-hand circular polarization; H, V – with horizontal and vertical linear polarization).

We take the q-plate with the charge q=1.5 (hereinafter $QP_{1.5}$). As mentioned earlier, usage of typical q-plate transform a Gaussian beam with a circular polarization to optical vortex with the topological charge $|l| = 3$:

$$\begin{aligned} \vec{e_L} C_0 e^{-\rho^2} &\to \vec{e_R} C_3 \rho^3 e^{i3\varphi - \rho^2}, \\ \vec{e_R} C_0 e^{-\rho^2} &\to \vec{e_L} C_3 \rho^3 e^{-i3\varphi - \rho^2}. \end{aligned} \tag{3}$$

In our analysis of a light wave transformed by $QP_{1.5}$ with a phase core the total complex intensity is considered as a sum of complex amplitudes for the Laguerre-Gauss modes with the azimuthal indices $l = 0$ and $l = \pm 3$, corresponding to the TEM_{00} mode (noise due to the presence of a nonsingular region in the centre of the element – Gaussian beam, Fig.2, *c*) and the TEM_{03} mode (vortex with the topological charge $|l| = 3$). In this case the transformation of the light-wave amplitude in accordance with formulae (2), (3) may be given as:

$$\begin{aligned} \vec{e_L}\, LG_0(L) &\to e^{-\rho^2}\left(C_0 \vec{e_L} + \vec{e_R}\, C_3 \rho^3 e^{i3\varphi}\right), \\ \vec{e_R} LG_0(R) &\to e^{-\rho^2}\left(C_0 \vec{e_R} + \vec{e_L}\, C_3 \rho^3 e^{-i3\varphi}\right). \end{aligned} \tag{4}$$

Vector Vortex Beams

For experimental study of the polarization singularity, we consider linearly polarized Gaussian radiation of a He–Ne laser passing through $QP_{1.5}$. Figure 3 shows photographs of the intensity profiles for the transformed beam at two orthogonal polarization orientations of input radiation. Spatial intensity distribution reveals three dips instead of one, pointing to complexity of its polarization structure.

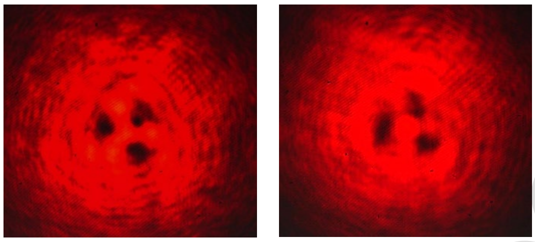

a *b*

Figure 3 – Photographs of the formed beam profiles.
Input beam polarization: *(a)* – horizontal, *(b)* – vertical.

Based on expression (4), we can write an expression for the complex field amplitude of linearly polarized radiation transformed on its passage through the q-plate. To take into account the polarization state of a light beam entering the q-plate, we express vector state of light in terms of the combinations of linear and circular polarizations as follows:

$$H = \frac{L+R}{\sqrt{2}},\ V = \frac{i(R-L)}{\sqrt{2}}, \tag{5}$$

$$R = \frac{H-iV}{\sqrt{2}}, L = \frac{H+iV}{\sqrt{2}},$$

where H and V – linear horizontal and vertical polarizations, R and L – right-hand and left-hand circular polarizations, respectively.

When a horizontally polarized beam passes through $QP_{1.5}$, the complex field amplitude, taking into account (4), (5), is determined by the expression:

$$LG_{\mathrm{q}=1,5}\,(H) = e^{-\rho^2}\left(C_0\overrightarrow{e_H} + \rho^3 C_3 \frac{\overrightarrow{e_R}\,e^{i3\varphi}+\overrightarrow{e_L}e^{-i3\varphi}}{\sqrt{2}}\right). \tag{6}$$

In the case of vertically polarized light we have

$$LG_{\mathrm{q}=1,5}\,(V) = e^{-\rho^2}\left(C_0\overrightarrow{e_V} - \rho^3 C_3 i \frac{\overrightarrow{e_R}\,e^{i3\varphi}-\overrightarrow{e_L}e^{-i3\varphi}}{\sqrt{2}}\right) \tag{7}$$

or

$$LG_{\mathrm{q}=1,5}\,(H) = \overrightarrow{e_H}e^{-\rho^2}(\,C_0 + C_3\rho^3 \mathrm{Cos}[3\varphi]) + \overrightarrow{e_V}e^{-\rho^2}C_3\rho^3\ \mathrm{Sin}[3\varphi], \tag{8}$$

$$LG_{\mathrm{q}=1,5}\,(V) = \ \overrightarrow{e_V}e^{-\rho^2}(\,C_0 - C_3\rho^3 \mathrm{Cos}[3\varphi]) + \overrightarrow{e_H}e^{-\rho^2}C_3\rho^3\ \mathrm{Sin}[3\varphi]. \tag{9}$$

The polarization topology of a singular beam was analyzed considering transmission of light through an analyzer. During analysis, the vector field geometry is characterized by the analyzer axis oriented perpendicular to the field vector of light entering the q-plate. At that equations (8), (9) take the following form:

$$LG^{\perp}_{q=1,5}(H) = e^{-\rho^2}\overrightarrow{e_V}C_3\rho^3\ \mathrm{Sin}[3\varphi], \tag{10}$$

$$LG^{\perp}_{q=1,5}(V) = e^{-\rho^2}\overrightarrow{e_H}C_3\rho^3\ \mathrm{Sin}[3\varphi]. \tag{11}$$

When the analyzer axis direction is coincident with the field vector direction for the input light field, expressions (8), (9) are changed as follows:

$$LG^{\parallel}_{q=1,5}(H) = \overrightarrow{e_H} e^{-\rho^2}(C_0 + C_3\rho^3 Cos[3\varphi]), \tag{12}$$

$$LG^{\parallel}_{q=1,5}(V) = \overrightarrow{e_V} e^{-\rho^2}(C_0 - C_3\rho^3 Cos[3\varphi]). \tag{13}$$

According to equations (10) – (13), when there is no noise in a singular polarization beam ($C_0 = 0$), its intensity is sinusoidally varying about the centre, forming $4q$ light spots. The light-beam distribution patterns for horizontal and vertical polarization modes entering the q-plate are rotated relative to each other about the centre by π/3. Sum field of orthogonal polarization modes transmitted through the element looks like a classical doughnut, with the characteristic intensity dip at the centre. Noise arising in a singular beam leads to the transformation of the intensity distribution over the beam profile when light passes through an analyzer, in line with formulae (12), (13). When the analyzer axis direction is coincident with the direction of the field vector entering the q-plate, the intensity distribution pattern no longer has the characteristic dip at the beam centre.

Based on expressions (8) – (13), we have calculated the intensity distribution over the vector beam profile and the polarization topologies. To include contributions made by nonsingular and singular components in an optical beam, in the process of cacluating the normalized amplitudes were given for the Gaussian component as $C_0 = \sin\delta$ and for the amplitude of a singular beam – as $C_3 = \cos\delta$. Figure 4 presents the calculation results for the intensity distribution of transformed light in the absence of an analyzer (*a*) and after passage through the analyzer, oriented in parallel (*b*) or perpendicularly (*c*) to the input linear polarization. The patterns were calculated for different noise

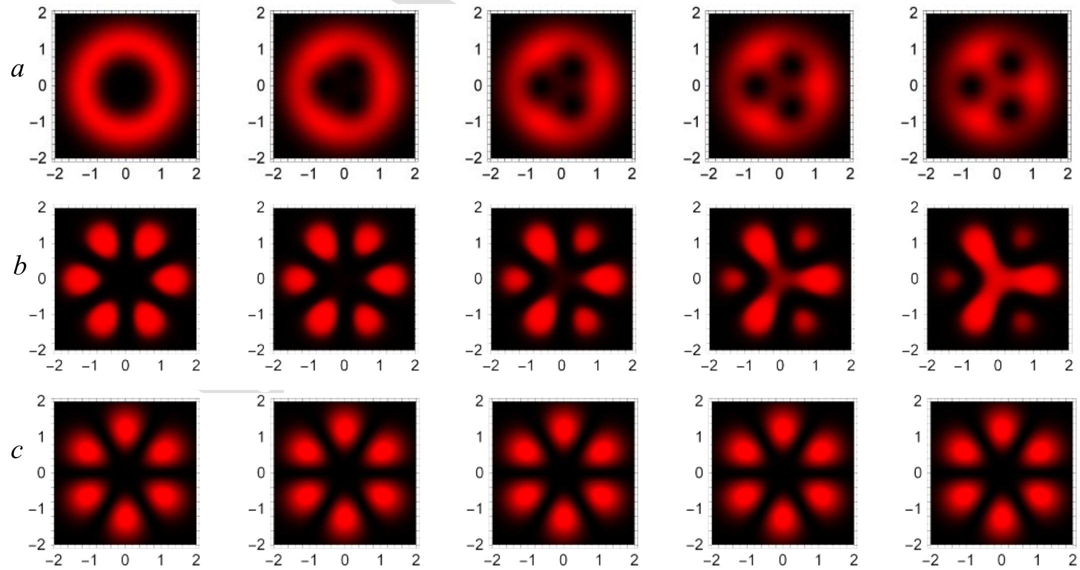

Figure 4 – The calculated intensity distributions for transformed light in the absence of an analyzer (*a*) and after passage through the analyzer, oriented in parallel (*b*) or perpendicular (*c*) to the input linear polarization (from left to right: δ = 0, π/32, π/16, 3π/32, π/8).

fractions depending on the δ. As demonstrated by the results, coherent Gaussian noise influences the polarization topology in a singular vortex.

Theoretical analysis of the intensity distribution over the light-beam profile reveals three dips (Fig. 4, *a*) as noise is involved. The number of dips at the intensity profile is associated with a topological charge of the formed vector vortex ($l_p = 3$), whereas spatial localization is determined by different amplitudes of noise C_0 and of the vector vortex C_3. The greater the noise amplitude C_0, the further the intensity dips from the centre and the more clearly defined at the light-beam profile. The first column at the left in Figure 4 shows the intensity distribution for a polarization vortex in the absence of noise and with the charge $l_p = 3$.

Figure 5 presents the experimental results for the polarization topology of a singular vortex beam excited by vertically polarized (Fig. 5, a) and horizontally polarized (Fig. 5, b) light passing through $QP_{1.5}$. Beam profile intensity distributions were recorded at different values of the angle γ between the analyzer axis and the input polarization.

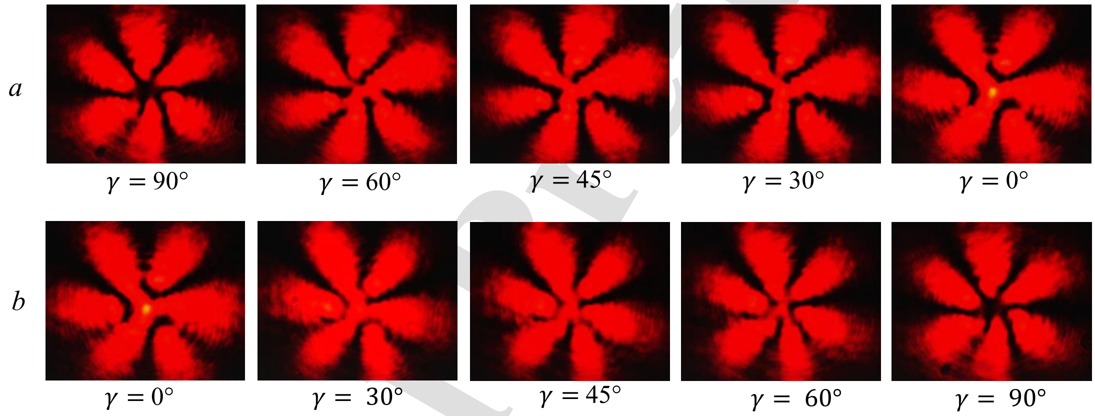

Figure 5 – Beam profile intensity distribution for different relative orientation γ of the analyzer and polarization of input light for vertically (*a*) and horizontally (*b*) polarized input light.

It should be noted that the measured intensity distributions at the angle $\gamma = 0°$ are associated with the case demonstrated in Fig. 4, *b,* when the noise component is involved ($\delta = \pi/8$) and the analyzer is oriented parallel to the polarization of radiation entering $QP_{1.5}$. Thus, the proposed theoretical description of the formation of a vector singular beam using a model of q-plate with phase core is in good agreement with the experimental data and allows predicting the polarization topology of the formed beam.

For a detailed verification of the proposed theoretical interpretation, we have calculated the interference patterns of a vector vortex with a plane reference wave. The analysis was performed for the fields calculated according to (12), (13) at different amplitudes of the C_0 and C_3 components. Figure 6 shows interference patterns for horizontal and vertical polarization at the input of $QP_{1.5}$ at parallel (Fig. 6, *a*) and perpendicular (Fig. 6, *b*) relative orientation of the analyzer.

Figures 7 and 8 show the results of interference summation of the polarization vortex formed by $QP_{1.5}$ for different relative orientations of the polarization plane of the input field and the coherent plane wave.

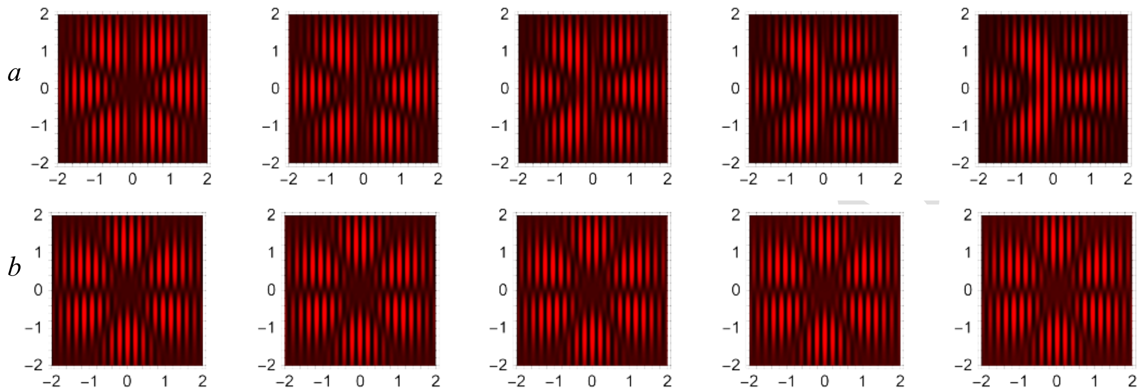

Figure 6 – The calculated interference patterns for a vector vortex with a plane reference wave: parallel (*a*) and perpendicular (*b*) orientations of the analyzer axis and the polarization of input light (noise level from left to right: δ = 0, π/32, π/16, 3π/32, π/8).

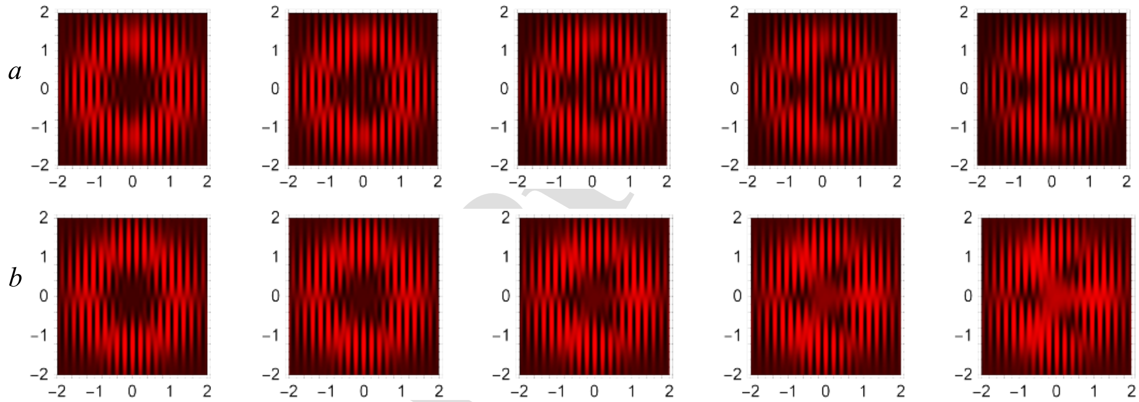

Figure 7 – The calculated interference patterns for a vector vortex with a plane reference wave: input and reference – horizontal polarization (*a*); input – horizontal, reference – vertical polarization (*b*) (noise level from left to right: δ = 0, π/32, π/16, 3π/32, π/8).

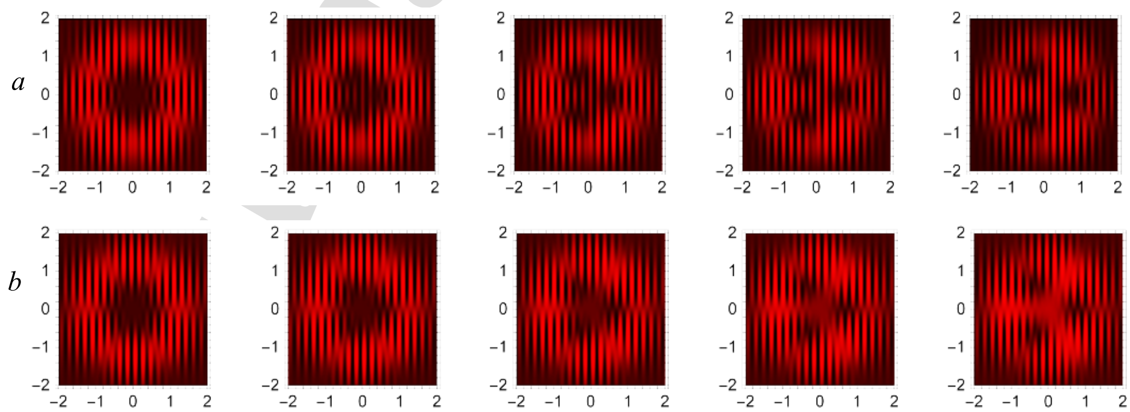

Figure 8 – The calculated interference patterns for a vector vortex with a plane reference wave: input and reference – vertical polarization (*a*); input – vertical, reference – horizontal polarization (*b*) (noise level from left to right: δ = 0, π/32, π/16, 3π/32, π/8).

As expected, in all analyzed cases (Figs. 6–8) the interference field exhibits no “forks” characteristic for phase singularities. The interference pattern of a beam with a polarization singularity is characterized only by the shift of interference fringes, pointing to complex polarization topology of the light beam.

Figure 9 shows the results of calculated and experimental interference patterns of vector vortices with a coherent reference wave in four cases of interaction geometry. The view of patterns on Fig. 9, *a* and Fig. 9, *b* does not depend on the orientation of the reference wave polarization. The view of patterns on Fig. 9, *c* and Fig. 9, *d* obtained without usage of an analyzer.

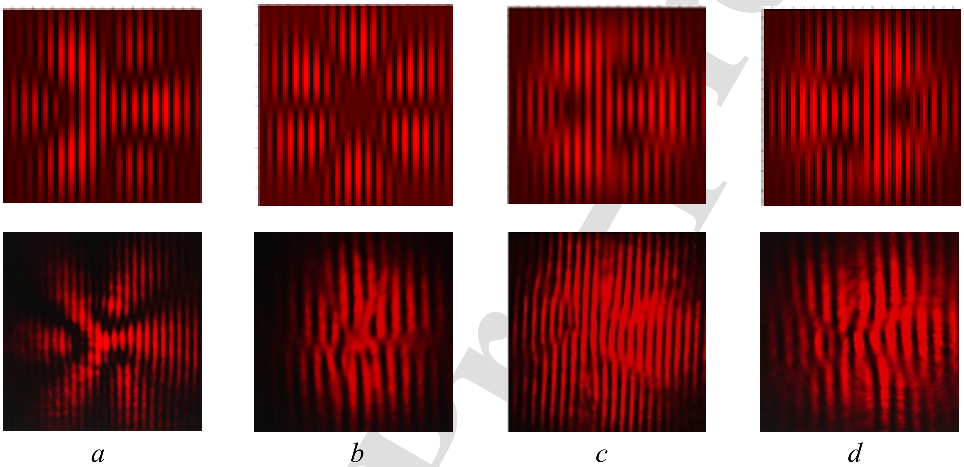

Figure 9 – Interference patterns of a vector vortex with a plane reference wave: parallel (*a*) and perpendicular (*b*) orientations of the analyzer axis and polarization of input light; input and reference wave – horizontal polarization (*c*), input and reference wave – vertical polarization (*d*). (The upper row presents the calculation results, lower – experimental data.)

Qualitative agreement between the results obtained during interference experiments and the calculation results derived based on the proposed model demonstrates its validity.

Optical Vortex Beams

The results of experimental studies of the intensity and phase distribution of a light beam, formed by passing of light with a circular polarization through $QP_{1.5}$ are given in Figure 10. In this case the beam profile also has three intensity dips (Fig.10, *a*). Interference analysis demonstrates the formation of three phase singularities with the charge $|l| = 1$ in beam profile (Fig.10, *b*). A sign of charge for the formed vortices (l=+1) is determined by the twist directions of the spiral formed in the interference pattern of an optical vortex with a linearly polarized spherical wave. Figure 10, *c* shows the patterns for each of the three phase singularities formed in the beam.

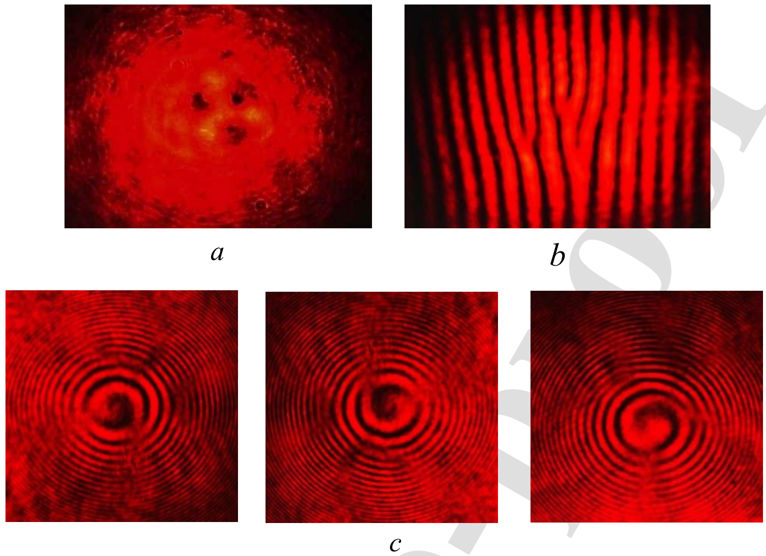

Figure 10 – The experimental results for an optical vortex formed on passage of left-hand circular beam through $QP_{1.5}$: beam profile intensity distribution (*a*); interference pattern with linearly polarized wave (*b*) and linearly-polarized spherical wave at every dip of the intensity (*c*).

Based on the proposed theoretical model, we have performed computer simulation of the coherent summation of the optical vortex beam formed by $QP_{1.5}$ with a plane reference wave (Fig.11). Similar to the previous section, analysis was performed for the fields calculated according to (4) at different amplitudes of the C_0 and C_3 components. The calculation takes into account the presence of the analyzer.

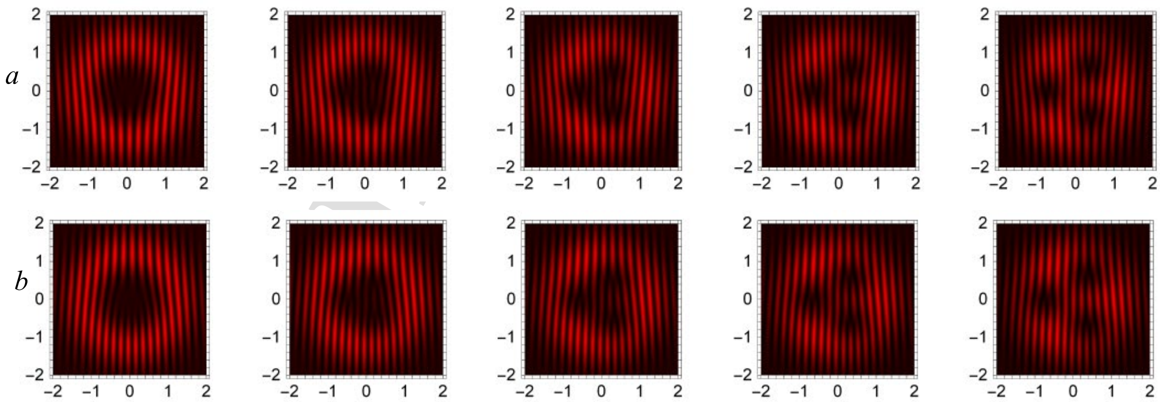

Figure 11 – The calculated interference patterns of a phase singular beam with a plane reference wave: input left-hand circular wave (*a*), input right-hand circular wave (*b*) (noise level from left to right: $\delta = 0, \pi/32, \pi/16, 3\pi/32, \pi/8$).

As seen in Fig.11, the beam profile reveals three phase singularities with the topological charge $|l| = 1$. A change in the circular-polarization rotation direction of light entering the element leads to changing a sign of charge which is confirmed by the change in the direction of the "fork" in the interference pattern.

To perform more detailed analysis of the phase topology of the received beam and to verify the proposed theoretical model for its description, we performed a computer simulation of the coherent summation of a phase singular beam with a plane wave upon changing the polarization state of light entering the $QP_{1.5}$. In the process the polarization direction was changing from the left-hand circular to the right-hand circular by means of changes in the ellipticity parameter. Formally, such a change in the polarization state of light may be included if we write the phase-vortex complex amplitude $LG_{1,5}$ as a superposition of two singular beams:

$$LG_{1,5} = \cos(\varepsilon)\left(e^{-\rho^2}\sin(\delta)\,\vec{e}_L + e^{-\rho^2+3i\varphi}\rho^3\cos(\delta)\,\vec{e}_R\right) + \\ +\sin(\varepsilon)\left(e^{-\rho^2}\sin(\delta)\,\vec{e}_R + e^{-\rho^2-3i\varphi}\rho^3\cos(\delta)\,\vec{e}_L\right), \quad (14)$$

where the parameter ε enables one to control the polarization state of radiation entering the q-plate. The calculation takes into account the presence of the analyzer.

Comparison of the calculation and experimental results shown in Figure 12 demonstrates that the proposed theoretical model gives an adequate description for the obtained experimental data.

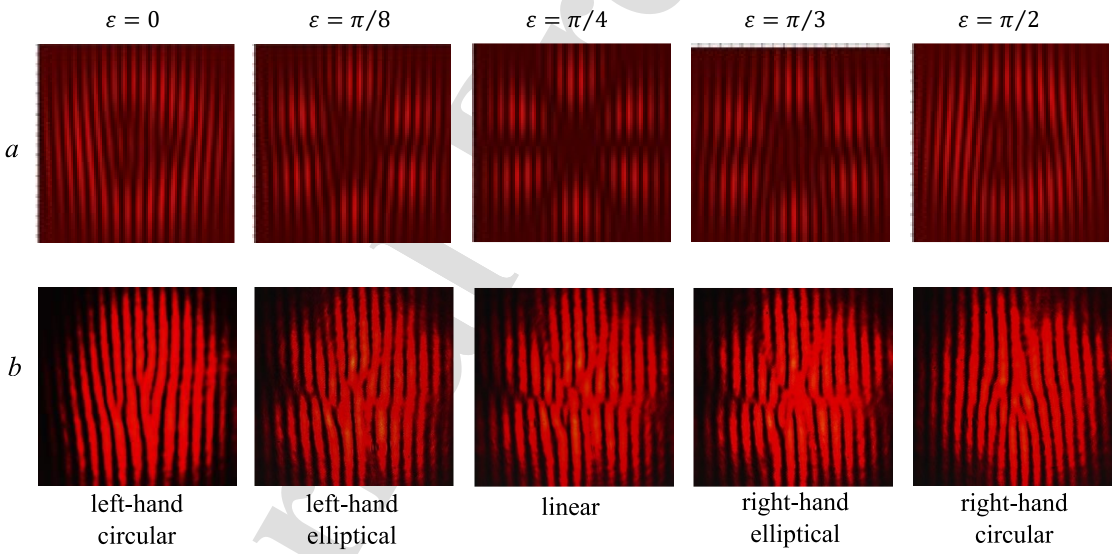

Figure 12 – Interference patterns of a phase singular beam with a plane reference wave: (a) – calculations (at the noise level $\delta = \pi/16$), (b) – experiment.

When the polarization state of radiation entering the q-plate is changing from the left-hand to the right-hand circular by means of changes in the ellipticity value, the "forks" characteristic for phase singularity in the interference pattern are broken. For $\varepsilon = \pi/4$, we get a state corresponding to a linear polarization and can observe the interference pattern characteristic for polarization singularity (compare with Fig.9, b). With further changing of the polarization state of input radiation, the forks begin to restore, completely appearing in the interference field with the inverted direction orientation when a sign of its spin orbital momentum is changed $\varepsilon = \pi/2$.

Conclusion

The paper presents a new type q-plate with a phase core offering coherent division of the input beam energy into singular and nonsingular components, with their subsequent coherent summation. The proposed method of the LC director photoalignment enables one to fabricate q-plates with a Phase Core for formation of radiation with complex phase and polarization structure, including the formation of beams carrying arrays of a given number of singularities of the charge $l = 1$. Developed LC based q-plates are characterized by their simple construction and efficient implementation of the latest liquid crystal photoalignment technique. The proposed theoretical model is confirmed by experimental results and is able to predict the polarization-phase state of optical vortices for various interaction geometries of the polarization state of light passing through the proposed topological element. The developed devices can find applications in technologies based on the usage of light fields with a complex amplitude profile: structured illumination microscopy, information coding and transfer, optical security, microrheology.

Acknowledgements

This work was supported by the National Programs for Scientific Research of the Republic of Belarus "Photonics and Electronics for Innovation" (Project No. 1.14) and "Convergence-2025" (Project No. 3.02.5).

References

[1] T. Lei, M. Zhang, Y. Li, P. Jia, G. N. Liu, X. Xu, Z. Li, C. Min, J. Lin, C. Yu, H. Niu, and X. Yuan, "Massive individual orbital angular momentum channels for multiplexing enabled by Dammann gratings," Light: Science and Appl. **4**, e257 (2015).
[2] M. Woerdemann, C. Alpmann, M. Esseling, and C. Denz, "Advanced optical trapping by complex beam shaping," Laser Photonics Rev. **7**, 839–854 (2013).
[3] A. L. Tolstik, "Singular dynamic holography," Russian Phys. J. **58**, 1431–1440 (2016).
[4] S. M. Block, D. F. Blair, and H. C. Berg, "Compliance of bacterial flagella measured with optical tweezers," Nature **338**, 514–518 (1989).
[5] X. Yin, X. Chen, H. Chang, X. Cui, Y. Su, Y. Guo, Y. Wang, and X. Xin, "Experimental study of atmospheric turbulence detection using an orbital angular momentum beam via a convolutional neural network," in *IEEE Access* **7**, 184235–184241 (2019).
[6] V. Yu. Bazhenov, M. V. Vasnetsov, M. S .Soskin, "Laser beams with screw dislocations in their wavefronts," JETP Lett. **52**, 429 (1990).
[7] H. Rubinsztein-Dunlop *et al,* "Roadmap on structured light" J. Opt. **19,** 013001 (2017).
[8] M. R. Dennis, K. O'Holleran, M. J. Padgett, "Singular optics: Optical vortices and polarization singularities," Progress in Optics **53**, 293–363 (2009).
[9] S. C. Tidwell, D. H. Ford, W. D. Kimura, "Generating radially polarized beams interferometrically," Appl. Opt. **29**, 2234–2239 (1990).
[10] R. Oron, S. Blit, N. Davidson, A. A. Friesem, Z. Bomzon, E. Hasman, "The formation of laser beams with pure azimuthal or radial polarization," Appl. Phys. Lett. **77**, 3322–3324 (2000).

[11] K. Huang, P. Shi, G.W. Cao, K. Li, X.B. Zhang, and. Y.P. Li "Vector-vortex Bessel–Gauss beams and their tightly focusing properties," Opt. Lett. **36**(6), 888-890 (2011).
[12] F. Flossmann, U. T. Schwarz, M. Maier, M. R. Dennis, "Polarization singularities from unfolding anoptical vortex through a birefringent crystal," Phys. Rev. Lett. **95**, 253901–4 (2005).
[13] Y. Kozawa, S. Sato, "Generation of a radially polarized laser beam by use of a conical Brewster prism," Opt. Lett. **30**, 3063–3065 (2005).
[14] Y. Shen, X. Wang, Z. Xie, C. Min, X. Fu, Q. Liu, M. Gong, and X. Yuan, "Optical vortices 30 years on: OAM manipulation from topological charge to multiple singularities," Light Sci. Appl. **8:90**, 1–29 (2019).
[15] E. Melnikova, D. Gorbach, I. Rushnova, V. Kabanova, S. Slusarenko, A. Tolstik, C. Losmanschii, A. Meshalkin, E. Achimova, "Optical vortices generation by azopolymeric relief gratings," Nonlinear Phenom. Complex Syst. **24**, 104–111 (2021).
[16] L. Marrucci, C. Manzo, and D. Paparo, "Optical spin-to-orbital angular momentum conversion in inhomogeneous anisotropic media," Phys. Rev. Lett. **96**, 163905 (2006).
[17] V. G. Chigrinov, "Liquid Crystal Photonics: Engineering Tools, Techniques and Tables" Nova Science Pub Inc. (2014).
[18] M. Peccianti, A. Dyadyusha, M. Kaczmarek, and G. Assanto, "Tunable refraction and reflection of self-confined light beams," Nature Phys. **2**, 737–742 (2006).
[19] A. A. Komar, A. L. Tolstik, E. A. Melnikova, and A. A. Muravsky, "Optical switch based on the electrically controlled liquid crystal interface," Appl. Opt. **54**, 5130–5135 (2015).
[20] E. A. Melnikova, A. L. Tolstik, I. I. Rushnova, O. S. Kabanova, and A. A. Muravsky, "Electrically controlled spatial-polarization switch based on patterned photoalignment of nematic liquid crystals," Appl. Opt. **55**, 6491–6495 (2016).
[21] Z. He, F. Gou, R. Chen, K. Yin, T. Zhan, and S.-T. Wu, "Liquid crystal beam steering devices: principles, recent advances, and future developments," Crystals **9**, 292 (2019).
[22] O. S. Kabanova, I. I. Rushnova, E. A. Melnikova, A. L. Tolstik, A. A. Muravsky, An. A. Murauski, R. Heintzmann, "Two-dimentional diffractive optical structure based on patterned photoalignment of polymerizable liquid crystal," J. BSU. Phys. **3**, 4–11 (2019).
[23] S. A. Nazarov, D. V. Gorbach, E. A. Mel'nikova, S. N. Kurilkina, and A. L. Tolstik, "Spin-orbit transformation of Bessel light beams by electrically controlled liquid-crystal elements," J. Opt. Technol. **85**, 189–192 (2018).
[24] L. Marrucci, E. Karimi, S. Slussarenko, B. Piccirillo, E. Santamato, E. Nagali and F. Sciarrino, "Spin-to-orbital optical angular momentum conversion in liquid crystal "q-plates": classical and quantum applications," Mol. Cryst. Liq. Cryst. **561**, 48–56 (2012).
[25] L. Marrucci, "The q-plate and its future," J. Nanophotonics. **7**, 078598-1–4 (2013).
[26] Y.-H. Huang, S.-W. Ko, M.-S. Li, S.-C. Chu, and A. Y.-G. Fuh, "Modulation of shape and polarization of beam using a liquid crystal q-plate that is fabricated via photo-alignment," Opt. Express. **21**, 10954–10961 (2013).
[27] Q. Wang, C.-H. Tu, Y.-N. Li, et al. "Polarization singularities: Progress, fundamental physics, and prospects," APL Photonics **6**, 040901 (2021).
[28] D. Lee, H. Lee, L. K. Migara, K. Kwak, V.P. Panov, J.-K. Song, "Widely Tunable Optical Vortex Array Generator Based on Grid Patterned Liquid Crystal Cell," Adv.Opt.Mat., **9(2)**, 2001604 (2021).

[29] Ruchi, S. K. Pal, and P. Senthilkumaran, “Generation of V-point polarization singularity lattices,” Optics Express, **25(16)**, 19326-19331 (2017).
[30] D.L. Andrews. Structured Light and Its Applications: An Introduction to Phase-Structured Beams and Nanoscale Optical Forces Academic Press; 1st edition (2008), 400p.
[31] S. Slussarenko, An. Murauski, Tao Du, V. Chigrinov, L. Marrucci, E. Santamato, “Tunable liquid crystal q-plates with arbitrary topological charge,” Opt. Express. **19**, 4085–4090 (2011).
[32] E. Hasman, G. Biener, A. Niv, and V. Kleiner, “Space-variant polarization manipulation,” Prog. Opt. **47**, 215–289 (2005).
[33] G. Biener, A. Niv, V. Kleiner, and E. Hasman, “Formation of helical beams by use of Pancharatnam-Berry phase optical elements,” Opt. Lett. **27**, 1875–1877 (2002).
[34] W. Ji, C.-H. Lee, P. Chen, W. Hu, Y. Ming, L. Zhang, T.-H. Lin, V. Chigrinov, and Y.-Q. Lu, “Meta-q-plate for complex beam shaping,” Sci. Rep. **6**, 25528 (2016)
[35] M. N. Miskiewicz and M. J. Escuti, “Direct-writing of complex liquid crystal patterns,” Opt. Express. **22**, 12691–12706 (2014).
[36] H. Larocque, J. Gagnon-Bischoff, F. Bouchard, R. Fickler, J. Upham, R. W. Boyd and E. Karimi, “Arbitrary optical wavefront shaping via spin-to-orbit coupling,” J. Opt. **18**, 124002 (2016).
[37] V. S. Mikulich, An. A. Murauski, Al. A. Muravsky, V. E. Agabekov, “Influence of methyl substituents on azo-dye photoalignment in thin films,” J. Appl. Spectrosc. **83**, 115–120 (2016).
[38] I. I. Rushnova, E. A. Melnikova, A. L. Tolstik, and A. A. Muravsky, “Electrically switchable photonic liquid crystal devices for routing of a polarized light wave,” Opt. Commun. **413**, 179–183 (2018).
[39] I. I. Rushnova, E. A. Melnikova, O. S. Kabanova, A. L. Tolstik, and A.A.Muravsky, “Fringe field-tunable LC refractive index interface for in-plane beam steering applications,” Appl. Opt. **59**, 10695-10699 (2020).
[40] A. A. Muravsky, A. A. Murauski, I. N. Kukhta, “Photoinduced hole dipoles’ mechanism of liquid crystal photoalignment,” Appl. Opt. **59**, 5102–5107 (2020).
[41] A. A. Muravsky, A. A. Murauski, I. N. Kukhta**,** A. S. Yakovleva, “High anchoring photoalignment material based on new photo-induced hole dipoles’ mechanism,” J. Soc. Inf. Displ. **29** 833–839 (2021).
[42] A. Muravsky, A. Murauski, “Effect of birefringent alignment layer on azimuthal anchoring energy measurement,” SID Int. Symp. Dig. Tech. Pap. **52** (S2), 497–499 (2021).
[43] I. V. Basistiy, V. Yu. Bazhenov, M. S. Soskin, and M. V. Vasnetsov, “Optics of light beams with screw dislocations,” Opt. Commun. **103**, 422–428 (1993).
[44] M. S. Soskin, V. N. Gorshkow, M. V. Vasnetsov, J. T. Malos, and N. R. Heckenberg, “Topological charge and angular momentum of light beams carrying optical vortices,” Phys. Rev. A. **56**, 4064–4075 (1997).
[45] T. Ando, N. Matsumoto, Y. Ohtake, Y. Takiguchi, and T. Inoue, “Structure of optical singularities in coaxial superpositions of Laguerre-Gaussian modes,” J. Opt. Soc. Am. A. **27**, 2602–2612 (2010).
[46] E. Karimi, G. Zito, B. Piccirillo, L. Marruci, and E.Santamato, “Hypergeometric-Gaussian modes,” Opt. Lett. **32**, 3053–3055 (2007).
[47] V.V. Kotlyar and A. A. Kovalev, “Family of hypergeometric laser beams,” J. Opt. Soc. Am. A. **25**, 262–270 (2008).

We subjected the article to a revision.

Corrections were made to the abstract, introduction, and conclusion in accordance with the reviewers' comments.

Data for comparison of results with other authors have been added to the "Scheme for recording q-plates with a central phase core" section.

Figures have been corrected. CF-755 Plot data File accordingly was changed.

Appropriate references have been added.

Declaration of interests

☒ The authors declare that they have no known competing financial interests or personal relationships that could have appeared to influence the work reported in this paper.

☐ The authors declare the following financial interests/personal relationships which may be considered as potential competing interests: